A MODEL FOR THE DYNAMIC INTRAGRANULAR FISSION GAS SWELLING AND RELEASE

J. M. GRIESMEYER, N. M. GHONIEM, D. OKRENT

Chemical, Nuclear and Thermal Engineering Department, School of Engineering and Applied Science, University of California, Los Angeles, California 90024, U.S.A.

Abstract

A Dynamic Intragranular Gas Release and Swelling Computer code (DIGRAS) has been developed to study the behavior of intragranular fission gas in mixed oxides during steady irradiations and in transients. The code models the interactions of non-equilibrium gas bubbles and the dynamic behavior of point defects. A variety of rate processes have been included in the model, such as bubble nucleation, re-solution, coalescence and gas migration to grain surfaces. The describing equations have been simplified using grouping and partitioning techniques. Steady irradiation simulation results agree reasonably well with experimentally measured gas release. On the other hand, simulating recent thermal transient experiments indicated that the final intragranular swelling is strongly dependent on fuel stoichiometry. Bubble diffusion rates are found to strongly affect the bubble distribution and potential for fuel motion. However, the final swelling was only weakly dependent upon bubble diffusion rates.

I. Introduction

Swelling due to the retained fission gas is a major factor in the closure of the fuel-clad gap and subsequent loads to the cladding. Gas in the plenum of the fuel pin can also cause loads to cladding if the gap is open. Fission gas pressure in the plenum or in the fuel itself provides a driving force for fuel disruption and dispersal once the clad has failed. Understanding fission gas effects requires fundamental data and modeling of microscopic phenomena. The modeling is used to interpret the data and discover important parameters of fission gas behavior as well as to extrapolate from scarce and often non-prototypic data to the actual or anticipated situation.

The Dynamic Intragranular Gas Release and Swelling code (DIGRAS) has been developed at UCLA to study and identify important variables in the behavior of intragranular fission gas in mixed oxide fuel [1]. Previous investigations at UCLA [2] indicated that the fission gas bubbles do not maintain an equilibrium size during a transient because the migration of point defects is too slow to allow the bubble expansion to its equilibrium size as the temperature increases or after coalescence. Recent HEDL experimental evidence is in basic agreement with this finding [3]. Following work indicated that the point defects have to be treated dynamically as they do not maintain their thermal equilibrium concentrations during a transient [4]. Also, during steady-state irradiations at normal operating temperature, the fission produced point defects result in concentrations many orders of magnitude above the thermal equilibrium values. The DIGRAS code models the intragranular behavior of fission gas explicitly treating gas bubble interactions and the dynamic behavior of point defects. This paper describes the model and illustrates some of its applications.

2. Description of the DIGRAS Model

2.1 Main Features

(1) A rate theory approach provides a convenient method to study the space averaged behavior of the fission gas cavities, gas atoms, and point defects. The rate equations are material balance equations between production and loss of each species. The basic assumption is that a discrete random array of sinks for point defects, gas atoms or gas bubbles can be approximated as an effective medium with appropriate sink desnities and strengths.

(2) In order to reduce the number of rate equations, the bubble distribution is grouped according to gas content while the character of the distribution is preserved by approximately conserving its radial moment and the first moments about N.

(3) Fuel stoichiometry is taken into account and the point defect populations are explicitly treated.

(4) Efficient integration of the resulting rate equations is used to reduce computational expense and improve accuracy.

(5) In order to facilitate sensitivity studies, the model is flexible and interpretation of results is made easier by detailed reporting of the rate processes.

2.2 Treatment of Physical Phenomena

2.2.1 Nucleation

Nucleation rates of gas bubbles are calculated by either a homogeneous or heterogeneous mechanism. In the homogeneous case the nucleation rate is related to the rate at which gas atoms randomly come together to form a digas cluster. The heterogeneous mechanism assumes that the single gas atoms in the wake of fission fragments are nucleated to form bubbles containing a fixed number of gas atoms.

2.2.2 Re-Solution

The solubility of gas atoms in the fuel matrix is enhanced during irradiation by fission fragments that knock gas out of bubbles and back into the matrix. It is modeled here by one or both of two mechanisms: the Turnbull type mechanism [5] which assumes that the bubbles in the path of the fission fragment can be completely destroyed, and the Nelson mechanism [6] in which single gas atoms are knocked out of the gas bubble when given enough energy in a collision with the fission fragment.

2.2.3 Coalescence

Coalescence by random migration is modeled using the standard colloidal coalescense rates of Chandrasekhar [8]. On the other hand, coalescence of bubbles moving in a temperature gradient is obtained using their geometrical cross-sections and the forces on the bubbles.

2.2.4 Gas Migration to Grain Surface

Single gas atom migration to the grain surface is modelled using rate theory. On the other hand, release of bubbles moving in a temperature gradient is approximated by assuming that the gas bubbles move in a block out of the grain with some average velocity.

2.3 Describing Equations

2.3.1 Concentration and Moment Rate Equations

Bubble interactions are determined by many irradiation and material variables. The combined effects of re-solution, coalescence and temperature variations result in a distribution of radii, $B_N(r,t)$, for bubbles containing N atoms. The bubble distribution is grouped according to the average gas content of the bubbles in a particular group. Formally the concentration of bubbles in group k with N_k atoms per bubble is

$$B_k(t) = \sum_N \int_0^\infty B_N(r,t)\, dr \qquad (1)$$

where the sum is over bubbles with N atoms within group k. The moment is defined by

$$M_k(t) = \sum_N \int_0^\infty r\, B_N(r,t)\, dr \qquad (2)$$

so that the average radius, r_k, of the bubbles in group k is

$$r_k = \frac{M_k}{B_k} \qquad (3)$$

The evolution of the gas distribution is determined by the integration of the equations for B_k and M_k. Therefore, the formal definitions are only used to derive approximations. The basic rate equation for the concentration in each group is

$$\frac{dB_k}{dt} = \frac{d}{dt}\left(\sum_{\substack{N \\ \text{in } k}} \int_0^\infty B_N\, dr\right) = \sum_j G_{kj} - \sum_j L_{kj} \qquad (4)$$

where the G_{kj} are the gain terms in group k due to the j interactions such as coalescence in the group below or re-solution in the group above k, the L_{kj} are the loss terms due to the various interactions. The moment rate equation is

$$\frac{dM_k}{dt} = \sum_{\substack{N \\ \text{in } k}} \int_o^\infty r \frac{dB_N}{dt} dr + \sum_{\substack{N \\ \text{in } k}} \int_o^\infty \frac{dr}{dt} B_N \, dr$$

$$\simeq \sum_j r_{kj} G_{kj} - r_k \sum_j L_{kj} + \left.\frac{dr}{dt}\right|_{r_k} B_k , \qquad (5)$$

where r_{kj} is the radius at which bubbles appear in group k due to the j interaction. For the loss terms it is assumed that the bubbles leave the group with the current average radius, r_k. However, when a bubble is produced containing N_g atoms and having radius, r_g, it will generally lie between two groups and must be partitioned.

The r_{kj} are determined by preserving the properties of the partitioned bubble. This is accomplished by either preserving the gas atom density or the radius ratio. Preserving gas atom density gives

$$r_{kj}^3 = N_k r_g^3 / N_g , \qquad (6)$$

While preserving the ratio of bubble radius to its equilibrium radius leads to

$$r_{kj} = r_{ek} r_g / r_{eg} . \qquad (7)$$

where r_{ek} and r_{eg} are the equilibrium radii of bubbles with N_k and N_g atoms, respectively.

The last term in equation (5) represents the change in the moment due to the volume adjustment of the bubbles by the flow of point defects. Solving the diffusion equation for the concentration of vacancies and interstitials outside the bubble and calculating the net flow of vacancies to and from the bubble leads to the expression

$$\frac{dr}{dt} = \frac{D_v}{r} (C_v - C_{vu} e^{-\Delta p \Omega / kT}) - \frac{D_i}{r} (C_i - C_{iu} e^{\Delta p \Omega / kT}) , \qquad (8)$$

where the $D_{v,i}$ are the metal vacancy/interstitial diffusion coefficients, $C_{v,i}$ are their ambient fractional concentrations, $C_{vu,iu}$ are the thermal equilibrium concentrations, Δp is the pressure misbalance between the gas in the bubble and the matrix forces, and Ω is the molecular volume of the fuel

2.3.2 Grouping and Bubble Partitioning

Individual rate equations are used for the first n bubble sizes. The equations are then grouped by a grouping factor, m, so that the average number of atoms in a group is given by

$$N_k = \begin{cases} k & k \leq n \\ mN_{k-1} & k > n \end{cases} \qquad (9)$$

When a bubble with N_g atoms is produced by an interaction, it is partitioned between two groups, $N_k \leq N_g < N_{k+1}$, and care must be taken to preserve as much of the original ungrouped distribution as is possible. In the present model, the zeroth and first moment of the discrete distribution are preserved. Letting f_k times the rate of production of bubbles with N_g atoms be the rate at which bubbles appear in group k, preservation of zeroth moment leads to

$$f_k N_k + f_{k+1} N_{k+1} = N_g , \qquad (10)$$

which clearly conserves the total number of gas atoms. Preserving the first moment is

equivalent to preserving the average N at which gas atoms of the partitioned bubble appear in the distribution and is expressed by the equation

$$f_k N_k^2 + f_{k+1} N_{k+1}^2 = N_g^2 \quad . \tag{11}$$

The set of constraints given by eqs. (10) and (11) give results that are independent of the grouping factor ($m \leq 6$). However, when the conservation of bubbles,

$$f_k + f_{k+1} = 1 \quad , \tag{12}$$

is used with conservation of atoms from eq. (10), as previously proposed [10], the results are strongly dependent upon the grouping factor. The constraints given by equaitons (10) and (12) were found to produce an artificial transfer of gas atoms into the larger bubble group.

2.3.3 Defect Rate Equations

We make the assumption that the fuel structure near the gas cavity surface is no different from the bulk (i.e., $UO_{2\pm x}$) so that the cavity kinetics is controlled by the slower moving uranium point defects. The time rate of change of the uranium vacancy and interstitial fractional concentrations, C_v and C_i are given by

$$\frac{dC_v}{dt} = P_{tot}^{ve} + P - P_{sv} - P_r \tag{13}$$

and

$$\frac{dC_i}{dt} = P_{tot}^{ie} + P - P_{si} - P_r \tag{14}$$

where $P_{tot}^{ve,ie}$ are the total metal defect emission rates from the microstructural sinks including the gas cavities, dislocations and grain boundaries. The $P_{sv,si}$ are the total defect loss rates to the microstructural sinks, P_r is the mutual recombination rate of the metal defects given by $\alpha C_v C_i$ where α is the recombination coefficient. P is the production rate of point defects.

2.3.4 Solution of the Rate Equations

The rate equations describing point defects (eq. (13) and eq. (14)) with the rate equations for each group (eq. (4) and eq. (5)) are assembled for integration in vector notation as

$$\dot{\bar{Y}} = \bar{f}\,(\bar{Y},t) \tag{15}$$

where t is time. Each component responds to environmental variations according to its own time scale which is in turn dependent upon temperature and microstructure. Systems with widely varying time constants pose problems for most integration schemes since most methods are stable for time steps on the order of the smallest time scale of the system, while interest is often focused on the longest live phenomena.

DIGRAS contains the Gear package which is ideally suited for solving such stiff systems of equations [8]. The main feature of the Gear package is its ability to take time steps on the order of the instantaneous time scale of the system. Hence, short time steps are required only during the life of the short lived phenomena. After their decay, large time steps result in significant savings in computational expense.

3. Applications of DIGRAS

3.1 Steady State Irradiations

To illustrate the use of DIGRAS in steady-state simulations, a series of irradiations to a burnup of 4% at a fission rate of 3.84×10^{13} $cm^{-3} sec^{-1}$ ($280 w/cm^3$) were simulated for

comparison with recent HEDL experimental results [3]. Under steady-state conditions, release of gas from the grain is primarily by the migration of single gas atoms to the grain boundary. Figure (1) shows that simultations assuming either homogeneous or heterogeneous nucleation of gas bubbles can be made to fit the release versus temperature curve. However, the gas atom diffusion coefficients (which were obtained from the measurements reviewed by Lawrence [9]) differed by a few orders of magnitude. This clearly indicates the existence of more than one unique combination of input parameters that would reproduce the results of a particular experiment. It might be inferred however, that the activation energy for gas atom migration in the fuel pin examined at HEDL is on the order of 80 to 105 kcal per mole since both the heterogeneous and homogeneous nucleation models required activation energies of at least this magnitude to reproduce the extremely sharp temperature threshold for gas release.

3.2 Thermal Transient Simulations

Sections of the fuel pin that was examined by the HEDL group were subjected to thermal transients and post inspected for gas content and swelling [3]. DIGRAS simulations were performed for a sample that was heated at about 240°K/sec to a temperature of 2700°K, held there for ten seconds, then allowed to cool. The initial conditions used for the simulations were the appropriate steady-state simulation results. Figure (2) shows the results for the swelling due to intra-granular gas bubbles for various oxygen to metal ratios and the two bubble nucleation mechanisms. The swelling here is defined as

$$S = \sum B_k \frac{4\pi}{3} r_k^3 \qquad (16)$$

Also shown is the instantaneous potential swelling defined as the calculated swelling due to the gas bubbles using the equilibrium volumes instead of the actual volume.

$$S_p = \sum B_k \frac{4\pi}{3} r_{ek}^3 \qquad (17)$$

S_p is a crude measure of the potential increase in bubble volume as the fuel becomes weak near the fuel melting point. The swelling is seen to be strongly dependent upon the fuel oxygen to metal ratio which determines the migration rates of the point defects. The main difference between the heterogeneous and homogeneous nucleation results for O/M = 1.98 is the slightly smaller initial gas content at the start of the transient as calculated by the heterogeneous model for the steady state irradiation at 1190°K (see figure 1). It was also found that the swelling results after the thermal transient were almost independent of the bubble diffusion coefficient that was used. The controlling factor was found to be the migration rates of the point defects rather than bubbles. However, the bubble distribution and the potential swelling were greatly affected by bubble diffusion coefficient.

4. Conclusions

A model for the dynamic intragranular fission gas swelling and release has been developed primarily for the investigation of fuel behavior during hypothetical accidents. However, model flexibility allows application to steady-state irradiations as well as experiments simulating transients. Model results are independent of the mathematical parameters (e.g. the grouping factor) and were shown to agree with steady state experiments on fission gas release using an activation energy of 80-105 kcal/mole for single gas atom migration.

Code results for simulated thermal transients indicated that swelling is controlled primarily by the diffusion rates of the point defects, and therefore is dependent upon fuel stoichiometry. Bubble diffusion rates are found to strongly affect the bubble distribution

and potential for fuel motion. However, the realized swelling appears to be only weakly dependent upon bubble diffusion rates.

References

[1] GRIESMEYER, J. M., "Dynamic Non-Equilibrium Intragranualr Fission Gas Behavior", Ph.D. Thesis, University of California (1979).

[2] GRIESMEYER, J. M., OKRENT, D., "A New Model for Non-Equilibrium Fission Gas Behavior", Trans. Amer. Nucl. Soc., 27, p. 322 (1977).

[3] HINMAN, C. H., SLAGLE, O. D., "Ex-Reactor Transient Fission Gas Release Studies, Fuel Pin PNL-2-4", HEDL Report, HEDL TME 77-83, (May, 1978).

[4] GRIESMEYER, J. M., GHONIEM, N. M., "The Response of Fission Gas Bubbles to the Dynamic Behavior of Point Defects", J. Nucl. Materials, (in press).

[5] TURNBULL, J. A., CORNELL, R. N., "The Re-Solution of Fission-Gas Atoms from Bubbles During the Irradiation of UO_2 at an Elevated Temperature", J. Nucl. Materials, 41, pp. 156-160, (1971).

[6] NELSON, R. S., "The Stability of Gas Bubbles in an Irradiation Environment", J. Nucl. Materials, 31, pp. 153-161, (1969).

[7] CHADRASEKHAR, T. S., "Stochastic Problems in Physics and Astronomy", Rev. Mod. Physics, 1, p. 61, (1943).

[8] HINDMARSH, A. C., "GEAR: Ordinary Differential Equation System Solver", LLL Report, UCID-30001, Rev. 3, (December, 1974).

[9] LAWRENCE, G. T., "A Review of the Diffusion Coefficient of Fission-Product Rare Gases in Uranium Dioxide", J. Nucl. Materials, 71, pp. 195-208, (1978).

[10] REST, J., "GRASS-SST: A Comprehensive, Mechanistic Model for the Prediction of Fission-Gas Behavior in UO_2-Base Fuels During Steady-State and Transient Conditions", Argonne Report, ANL-78-53, p. 31 (June 1978).

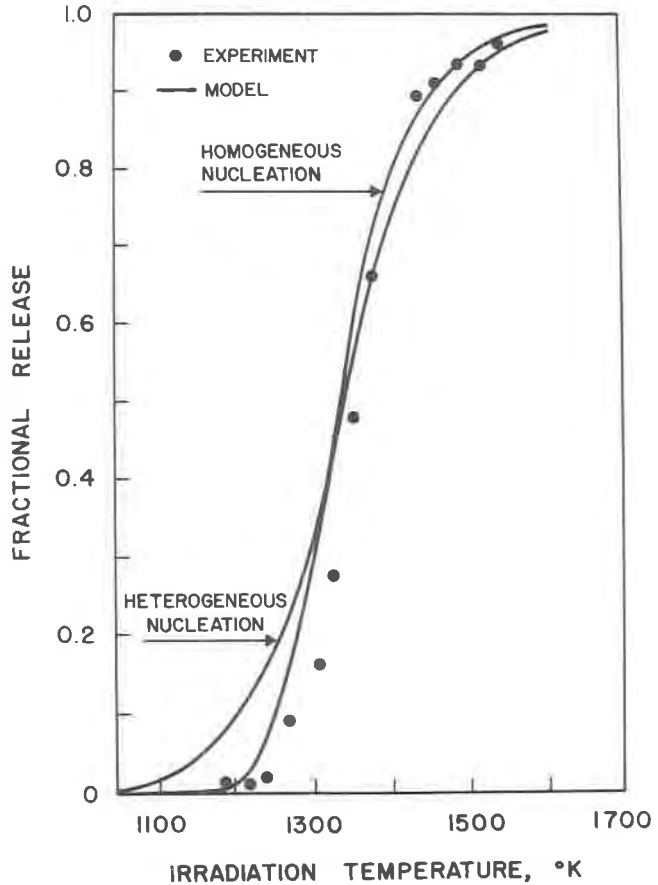
1.0
0.8
0.6
0.4
0.2
0
FRACTIONAL RELEASE
EXPERIMENT
MODEL
HOMOGENEOUS NUCLEATION
HETEROGENEOUS NUCLEATION
1100
1300
1500
1700
IRRADIATION TEMPERATURE, °K

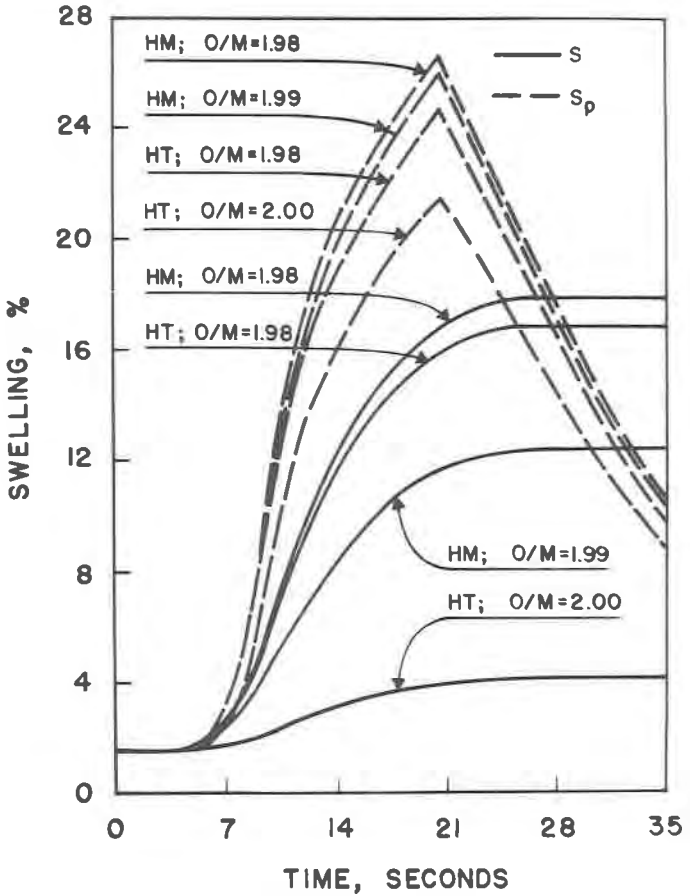
28
24
20
16
12
8
4
0
SWELLING, %
HM; O/M=1.98
HM; O/M=1.99
HT; O/M=1.98
HT; O/M=2.00
HM; O/M=1.98
HT; O/M=1.98
S
S_p
HM; O/M=1.99
HT; O/M=2.00
0
7
14
21
28
35
TIME, SECONDS